# Tracing effects of decalcification on solute sources in a shallow groundwater aquifer, NW Germany

Bettina A. Wiegand *

University of Goettingen, Geoscience Center – GZG, Goldschmidtstr. 3, 37077 Goettingen, Germany

SUMMARY

$\delta^{87}Sr$ values and Ca/Sr ratios were employed to quantify solute inputs from atmospheric and lithogenic sources to a catchment in NW Germany. The aquifer consists primarily of unconsolidated Pleistocene eolian and fluviatile deposits predominated by >90% quartz sand. Accessory minerals include feldspar, glauconite, and mica, as well as disperse calcium carbonate in deeper levels. Decalcification of near-surface sediment induces groundwater pH values up to 4.4 that lead to enhanced silicate weathering. Consequently, low mineralized Ca–Na–Cl- and Ca–Cl-groundwater types are common in shallow depths, while in deeper located calcareous sediment Ca–$HCO_3$-type groundwater prevails. $\delta^{87}Sr$ values and Ca/Sr ratios of the dissolved pool range from 7.3 to −2.6 and 88 to 493, respectively. Positive $\delta^{87}Sr$ values and low Ca/Sr ratios indicate enhanced feldspar dissolution in shallow depths of less than 20 m below soil surface (BSS), while equilibrium with calcite governs negative $\delta^{87}Sr$ values and elevated Ca/Sr ratios in deep groundwater (>30 m BSS). Both positive and negative $\delta^{87}Sr$ values are evolved in intermediate depths (20–30 m BSS). For groundwater that is undersaturated with respect to calcite, atmospheric supplies range from 4% to 20%, while feldspar-weathering accounts for 8–26% and calcium carbonate for 62–90% of dissolved $Sr^{2+}$. In contrast, more than 95% of $Sr^{2+}$ is derived by calcium carbonate and less than 5% by feldspar dissolution in Ca–$HCO_3$-type groundwater. The surprisingly high content of carbonate-derived $Sr^{2+}$ in groundwater of the decalcified portion of the aquifer may account for considerable contributions from Ca-containing fertilizers. Complementary tritium analyses show that equilibrium with calcite is restricted to old groundwater sources.

## Introduction

During the Pleistocene glaciations, eolian and fluvial sands were deposited over wide areas in Northern Europe (e.g. Ehlers et al., 1984; Eissmann, 2002; Walter, 2007). Today, the unconsolidated sediments represent economically important but vulnerable groundwater reservoirs that are exploited for drinking water supply. Particularly, unconfined aquifers, shallow water tables, and decalcification of soils increase the potential risk for environmental and anthropogenic contamination (e.g. Dahl and Dörhöfer, 1991; Dörhöfer et al., 2001).

Soils dominated by quartz sand have naturally low acid-neutralization capacities, and decalcification caused by natural and anthropogenic processes produces low pH values in shallow groundwater systems. As a consequence, the mobility of aluminum and other heavy metals increases, and leaching and transfer of toxic compounds may affect the quality of potable water resources. The effect of base cation loss on forested watersheds resulting from the impact of soil

acidification in Europe and North America was intensely studied throughout the past decades (e.g. Falkengren-Grerup et al., 1987; Shortle and Bondietti, 1992; Bricker and Rice, 1993; Likens et al., 1996; Lawrence et al., 1999; Huntington et al., 2000; Driscoll et al., 2001; Hrkal et al., 2006; Fenn et al., 2006).

$^{87}Sr/^{86}Sr$ and Ca/Sr ratios are useful natural tracers to discriminate sources of base cations and quantify inputs to hydrological systems (e.g. Bullen et al., 1996; Katz and Bullen, 1996; Probst et al., 2000; Wiegand et al., 2001; Négrel et al., 2004). Both tracers are reactive along flow paths and are controlled by the sources contributing to the dissolved $Sr^{2+}$ and $Ca^{2+}$ loads. While the Sr isotope composition is not affected by changes in $Sr^{2+}$ concentrations, the Ca/Sr ratios may be altered, e.g. by precipitation of secondary minerals and cation-exchange processes (e.g. Sposito, 1989; Capo et al., 1998).

In near-surface groundwater systems, dissolved $Sr^{2+}$ and $Ca^{2+}$ pools generally represent mixtures of atmospheric inputs and releases from mineral weathering. In addition, anthropogenic sources including fertilizers may be of importance (e.g. Böhlke and Horan, 2000; Soler et al., 2002; Vitòria et al., 2004). Under favorable conditions, the contributing sources have different Sr isotope and Ca/Sr ratios permitting the determination of origin

* Tel.: +49 551 3913234.
*E-mail address:* bwiegan@gwdg.de

and mixing proportions of solute inputs along flow paths. For example carbonate and silicate minerals are usually characterized by considerable differences in their isotope and concentration ratios. Studies focusing on experimental dissolution rates of Sr-bearing minerals include Åberg (1995), Brantley et al. (1998), and Taylor et al. (2000), while applications to water–rock interactions and weathering processes in the natural environment were reported by Miller et al. (1993), Johnson and DePaolo (1994), Bullen et al. (1997), Peterman and Wallin (1999), Quade et al. (2003), Jacobson et al. (2002), Bau et al. (2004), Shand et al. (2007) and others.

The present study is focused on a shallow groundwater aquifer located in Pleistocene siliciclastic deposits in NW Germany to assess changes in the chemical composition of the water caused by decalcification (carbonate dissolution) processes. A decrease in the acid-neutralization potential of soils and declining depths of decalcification are probably linked to a combination of natural and anthropogenic processes including fluctuating water tables, redox processes, agricultural exploitation, nitrification, acid rain deposition of the past decades, and increased groundwater withdrawal. Considerable variations in groundwater pH and alkalinity imply changes in the weathering regime across the aquifer. To trace the effects of decalcification on solute sources and quantify replenishing cation inputs from mineral and atmospheric sources, $^{87}Sr/^{86}Sr$ (here reported as $\delta^{87}Sr$ values) and Ca/Sr ratios of groundwater, rainwater, bulk sediment, and mineral separates were evaluated. A model for the evolution of groundwater with respect to the origin of dissolved $Ca^{2+}$ and $Sr^{2+}$ and quantification of solute fluxes from atmospheric and mineral sources is presented.

## Geology and hydrology

The water works of Ristedt is located about 10 km south of the city of Bremen in Lower Saxony, northwestern Germany (Fig. 1). About 20-million $m^3$ of groundwater are pumped annually from depths between 18 and 30 m for local drinking water supply by the Harzwasserwerke GmbH, Germany. The catchment area has a size of about 100 $km^2$, extending between the towns of Syke and Weyhe. The average yearly precipitation is 691 mm $yr^{-1}$ (source: Deutscher Wetterdienst/German Meteorological Service; www.dwd.de). Groundwater recharge is between 100 and 300 mm annually, corresponding to about 133-million $m^3 yr^{-1}$ (source: EG-WRRL Report 2005).

The aquifer is composed of Quaternary unconsolidated siliciclastic sediments (sands, intercalated with silt and gravel) that were deposited during the Pleistocene (mainly Elsterian and Saalian glaciations) (e.g. Ehlers et al., 1984; Grube et al., 1986; Meyer, 2005). In the northern catchment area, periglacial deposits created by solifluction during the Weichselian glaciation form a transition to sand-loess deposits in the south, and eolian sands in the west (Kartenserver des NIBIS, 2008a). Streams draining the catchment are bordered by peaty-clayey fens. Deposits of the northern catchment area show variable permeabilities from $>10^{-4}$ to $<10^{-5}$ m/s, while to the south medium permeabilities with coefficients between $10^{-5}$ and $10^{-4}$ m/s prevail. The western catchment surrounding the water works of Ristedt shows highest permeabilities of $>10^{-4}$ m/s (Kartenserver des NIBIS, 2008b). Groundwater drains largely through the streams Hache and Hombach both discharging to the river Weser.

Groundwater flows from the higher plains in the southwest (German "Geest") to the northeast (Weser marshlands) (Fig. 1). During the sampling campaign in summer 2001, the water table was between 20 and 25 m below the surface at the rim of the Geest plains, and between 1 and 4 m in the Weser marshlands. Groundwater in monitoring wells of the Geest is mostly oxic in contrast to the marshland where anoxic conditions prevail. Reducing conditions are linked to intercalations of organic-rich layers and coal fragments in the sand deposits. Alternating groundwater dynamics and redox processes in organic-rich sediments of the Weser marshland cause acidic conditions that contribute to natural decalcification of the soils.

## Methods

Groundwater samples ($n = 32$) were collected from monitoring wells in defined depths between 6 and 54 m below the soil surface (BSS). In addition, sediment from the unsaturated and saturated zone was collected (Fig. 1). In the unsaturated zone, sediment cores ranging between 2 and 5 m in depth were drilled with a piston corer. An additional core of 30 m length (B16) from the saturated zone located in the Weser marshlands was provided by the Harzwasserwerke GmbH. Water samples were filtered through 0.45 μm cellulose-nitrate filters, stabilized with 1% distilled $HNO_3$ and stored in pre-cleaned polyethylene bottles prior to analysis of Sr concentrations and $^{87}Sr/^{86}Sr$ ratios. A separate set of samples was collected for major elements and analyzed by standard procedures including ion-chromatography and graphite-AAS at the Central Laboratory of the Harzwasserwerke GmbH, Langelsheim, Germany. Saturation indices were modeled with the computer code PHREEQC (Parkhurst and Appelo, 1999). Tritium analyses were performed on 2 L of untreated groundwater samples using the liquid scintillation technique at the University of Goettingen, Germany. Selected samples were analyzed at the Hydroisotop GmbH, Germany.

Bulk sediment samples were dried (40 °C) prior to geochemical analysis. Selected sediment samples were pulverized and analyzed by X-ray fluorescence spectroscopy for major and trace components at the Geoscience Center, University of Goettingen, Germany. For Sr isotope analysis, about 100 mg of sediment powders were digested in a mixture of $HF–HNO_3–HCLO_4$ at 120 °C over night. The digestion of mineral separates ($\sim$10 mg) followed the same procedure. After complete dissolution and evaporation, the sample residue was dissolved in 6 N HCl at 120 °C and again evaporated. The sample residue was then re-dissolved in 2.5 N HCl for ion exchange chromatography. Separation of Sr from other cations was carried out on quartz glass columns using Biorad AG50 × 8 (200–400 mesh) resin and 2.5 N HCl. Groundwater ($\sim$10 mL) was pre-concentrated by evaporation before ion exchange chromatography. Sr concentrations were determined by isotope dilution technique using an $^{84}Sr$-enriched spike solution. Purified Sr fractions were loaded onto out-gassed Ta single filaments using 0.25 N $H_3PO_4$ and measured on a Finnigan MAT262 thermal ionization mass spectrometer (TIMS) at the Geoscience Center, University of Goettingen, Germany. $^{87}Sr/^{86}Sr$ ratios were corrected for instrumental fractionation using the natural $^{88}Sr/^{86}Sr$ ratio of 8.375209. Routine standard measurements yield $0.71026 \pm 0.00002 (2\sigma: n = 32)$ for the NBS987 Sr standard. Only distilled reagents were used for chemical sample preparation. Blanks were less than 0.5 ng for Sr. The reproducibility of the individual $^{87}Sr/^{86}Sr$ ratio is equal to or less than 0.00002 ($2\sigma$). All analyzed $^{87}Sr/^{86}Sr$ ratios were normalized to the average $^{87}Sr/^{86}Sr$ ratio of rainwater 0.710 (Wiegand et al., 2001) and are reported in delta notation according to the equation:

$$\delta^{87}Sr = \left( \frac{^{87}Sr/^{86}Sr_{sample}}{^{87}Sr/^{86}Sr_{rainwater}} - 1 \right) \times 1000 \qquad (1)$$

## Results

### Hydrogeochemical parameters

Changes in the physical and chemical properties across the aquifer (e.g. acid-neutralization capacity, redox conditions, resi-
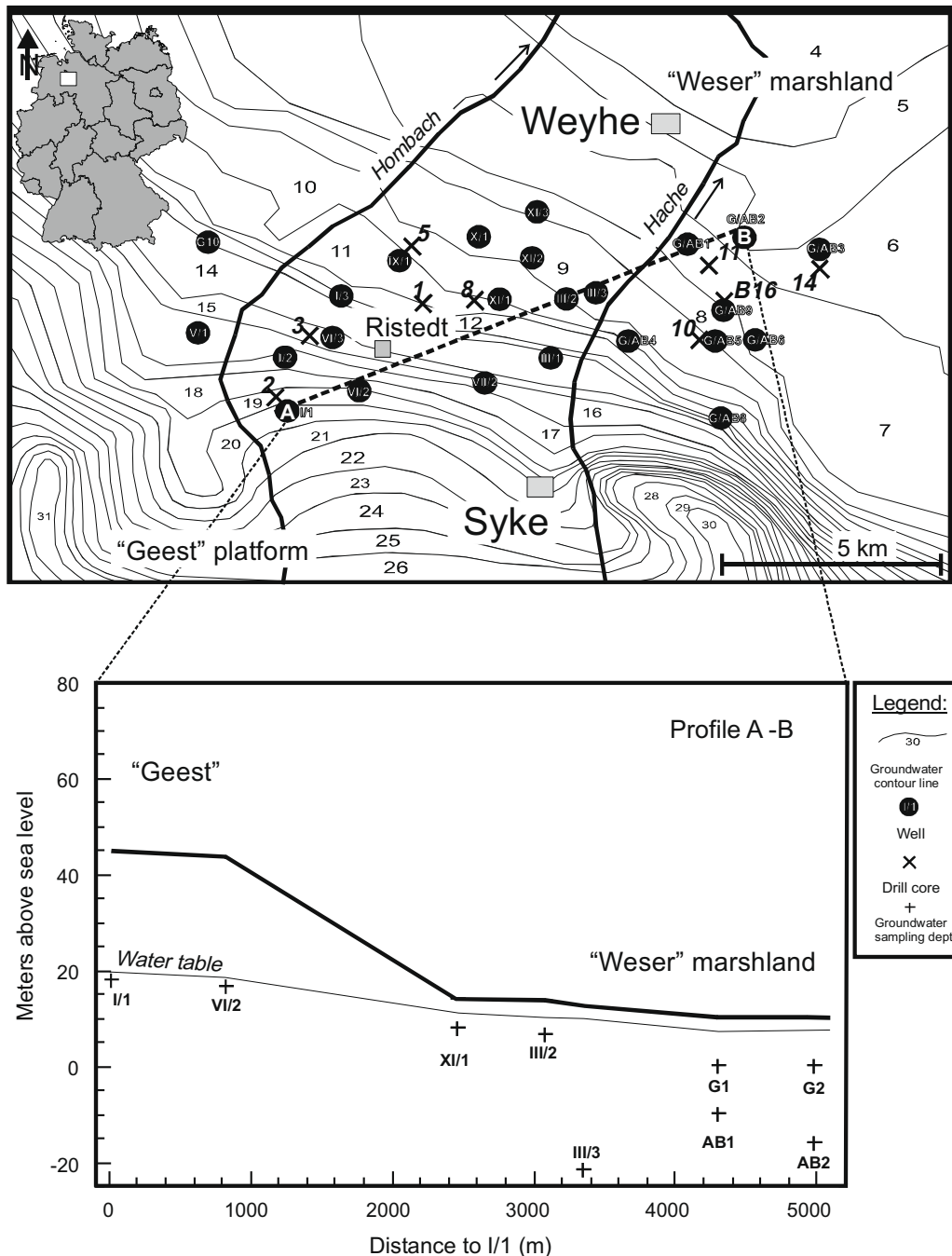
**Fig. 1.** Upper figure: distribution of groundwater contour lines in the catchment area surrounding the town of Ristedt (52°57′N; 8°46′E). The figure displays the locations of sampled wells (filled circles) and sediment cores (cross symbol with core number, see Table 2). Lower figure: cross section (A–B) of the aquifer in groundwater flow direction from the Geest platform to the Weser marshland. Cross symbols indicate sampling depths of wells across the profile.

dence times) produce a wide range in hydrological characteristics and solute concentrations in groundwater, e.g. total dissolved solids (85–393 mg/L), pH value (4.4–7.6), alkalinity (0.04–3.58 mmol/L), and dissolved oxygen content (0.1–11.2 mg/L). Concentration ranges of major solutes are: 4–91 mg/L $Na^+$, 1–93 mg/L $K^+$, 7–51 mg/L $Ca^{2+}$, 2–18 mg/L $Mg^{2+}$, 5–141 mg/L $Cl^-$, 5–154 mg/L $SO_4^{2-}$, and 2–218 mg/L $HCO_3^-$ (Table 1).

$Na^+$ and $Cl^-$ are positively correlated ($R^2 = 0.57$), and Na/Cl ratios (avg. = 0.52) of most groundwater samples are slightly below the Na/Cl ratio (=0.74) of local precipitation, probably as a result of cation-exchange processes involving $Na^+$. For $Na^+$ and $Cl^-$ a predominant atmospheric origin is assumed; only well XI-3 has an

elevated $Na^+$ (91 mg/L) and $Cl^-$ (141 mg/L) content, possibly due to anthropogenic contamination. Elevated $K^+$ concentrations and Mg/Ca ratios in some shallow and intermediate wells likely result from enhanced silicate weathering, especially in groundwater with low pH values. High dissolved $K^+$ concentrations may be an indicator for dissolution of K-rich silicate phases. $HCO_3^-$ is considerably depleted in those wells and increases with depth parallel increasing pH values. Depletion of $HCO_3^-$ and $Ca^{2+}$ in shallow wells are an indicator of sediment decalcification.

Moreover, the chemical composition of groundwater is affected by complex redox reactions. In the northwestern part of the aquifer (Weser marshlands), reducing groundwater conditions persist as a

**Table 1**
Hydrological data, concentrations of major- and trace elements, tritium, and $\delta^{87}Sr$ values of groundwater samples.

| Sample ID | Water table (m) BSS[a] | Well depth (m) BSS[a] | T°C | pH | ALK[a] (mmol/L) | TDS[a] (mg/L) | O$_2$ (mg/L) | Na (mg/L) | K (mg/L) | Ca (mg/L) | Mg (mg/L) | Fe (mg/L) | Sr (mg/L) | HCO$_3$ (mg/L) | Cl (mg/L) | SO$_4$ (mg/L) | NO$_3$ (mg/L) | SI$_{cc}$[b] | Tritium (TU) | Ca/Sr | $\delta^{87}Sr$[c] | $^{87}Sr/^{86}Sr$ |
|---|---|---|---|---|---|---|---|---|---|---|---|---|---|---|---|---|---|---|---|---|---|---|
| I/1 | 25.20 | 27 | 13 | 5.55 | 0.17 | 298 | 9.3 | 19.7 | 4.5 | 36.8 | 13.5 | 0.159 | 0.268 | 10.1 | 42.3 | 37.3 | 125.6 | −4.38 | 12 | 137 | 1.99 | 0.71141 |
| I/2 | 23.40 | 26 | 11.8 | 5.35 | 0.17 | 315 | 10 | 34.3 | 3.1 | 39.1 | 10.7 | 0.366 | 0.220 | 10.4 | 41.4 | 125.3 | 43 | −4.79 | 19 | 178 | 3.87 | 0.71275 |
| I/3 | 3.50 | 7 | 11.3 | 4.85 | 0.11 | 122 | 3.5 | 12.8 | 4.5 | 8.7 | 6.8 | 0.181 | 0.099 | 6.7 | 19.9 | 36.8 | 20.5 | −6.55 | 10 | 88 | 7.34 | 0.71521 |
| III/1 | 2.10 | 7 | 11.5 | 5.55 | 1.01 | 127 | 0.4 | 4.4 | 2.9 | 21.6 | 2.3 | 0.203 | 0.075 | 61.6 | 4.5 | 20.9 | 4.9 | −3.81 | 8 | 288 | 2.87 | 0.71204 |
| III/2 | 3.25 | 7 | 11.1 | 4.35 | 0.04 | 230 | 3.4 | 11.5 | 13.2 | 28.4 | 9.0 | 0.174 | 0.186 | 2.1 | 25.6 | 70.3 | 62.2 | −7.57 | 13 | 153 | 3.32 | 0.71236 |
| III/3 | 2.65 | 54 | 12.5 | 7.35 | 3.00 | 320 | 2.4 | 15.9 | 4.0 | 51.3 | 5.7 | 0.068 | 0.285 | 182.7 | 35.2 | 5.1 | 1.3 | −0.33 | <0.6 | 180 | −2.61 | 0.70815 |
| V/1 | 21.50 | 26 | 11.8 | 5.35 | 0.17 | 162 | 10.1 | 21.2 | 2.0 | 18.0 | 4.0 | 0.045 | 0.089 | 10.4 | 31.4 | 48.1 | 18.9 | −5.07 | 38 | 202 | 2.58 | 0.71183 |
| VI/2 | 25.10 | 27 | 12.6 | 5.45 | 0.14 | 293 | 10 | 22.4 | 4.5 | 37.8 | 11.5 | 0.068 | 0.178 | 8.5 | 44.6 | 58.5 | 96.7 | −4.65 | 23 | 212 | 2.28 | 0.71162 |
| VI/3 | 5.90 | 10 | 11.0 | 6.55 | 2.29 | 265 | 11.2 | 24.2 | 3.0 | 44.0 | 10.9 | 0.005 | 0.245 | 139.4 | 14.4 | 10.7 | 10.7 | −1.52 | 20 | 180 | 3.59 | 0.71255 |
| VII/2 | 14.70 | 16 | 11.8 | 5.3 | 0.10 | 255 | 10.8 | 11.4 | 10.3 | 24.0 | 17.3 | 0.091 | 0.271 | 5.8 | 21.6 | 45 | 113.9 | −5.3 | 12 | 89 | 6.13 | 0.71435 |
| IX/1 | 2.85 | 7 | 11.1 | 5 | 0.16 | 367 | 0.8 | 38.2 | 24.7 | 22.9 | 12.9 | 18.8 | 0.198 | 9.8 | 84 | 138.1 | 6.6 | −5.76 | 14 | 116 | 5.76 | 0.71409 |
| X/1 | 2.00 | 7 | 11.1 | 5.75 | 1.10 | 194 | 0.3 | 24.4 | 2.8 | 21.1 | 3.0 | 2.76 | 0.078 | 67.1 | 46.9 | 17.1 | <0.1 | −3.44 | 22 | 271 | 0.72 | 0.71051 |
| XI/1 | 3.30 | 6 | 10.9 | 4.55 | 0.07 | 247 | 1.5 | 26.7 | 9.5 | 25.2 | 8.7 | 5.07 | 0.198 | 4.3 | 54.8 | 86.5 | 18.2 | −6.94 | n.d. | 127 | 5.68 | 0.71403 |
| XI/2 | 4.95 | 8 | 11.0 | 4.5 | 0.05 | 314 | 9 | 37.3 | 7.4 | 27.7 | 15.5 | 0.017 | 0.229 | 2.7 | 55.7 | 96.6 | 62.9 | −7.21 | n.d. | 121 | 7.30 | 0.71518 |
| XI/3 | 4.40 | 9 | 11.3 | 4.75 | 0.11 | 377 | 5.2 | 90.7 | 14.7 | 18.7 | 3.7 | 0.054 | 0.086 | 6.7 | 141.2 | 48 | 45.8 | −6.46 | n.d. | 217 | 2.54 | 0.71180 |
| G1 | 2.65 | 10 | 10.9 | 5.65 | 0.48 | 299 | 0.1 | 13.9 | 33.8 | 37.4 | 7.0 | 4.30 | 0.124 | 29.3 | 37.5 | 129 | 0.3 | −3.82 | 23 | 302 | 1.87 | 0.71133 |
| G2 | 2.30 | 10 | 10.7 | 4.85 | 0.09 | 253 | 0.1 | 12.8 | 18.9 | 30.0 | 8.8 | 4.70 | 0.178 | 5.5 | 28.8 | 134.3 | 1.1 | −6.19 | 17 | 169 | 2.86 | 0.71203 |
| G3 | 1.45 | 10 | 10.8 | 5.3 | 0.21 | 353 | 0.7 | 34.2 | 18.4 | 30.7 | 14.8 | 12.7 | 0.297 | 12.5 | 66.5 | 153.9 | 0.3 | −4.96 | n.d. | 103 | 4.13 | 0.71293 |
| G4 | 4.05 | 14 | 11.6 | 5.2 | 0.19 | 286 | 6 | 31.7 | 12.2 | 23.9 | 13.3 | 0.060 | 0.217 | 11.3 | 50.1 | 69.2 | 67.5 | −5.26 | 17 | 110 | 6.14 | 0.71436 |
| G5 | 2.95 | 11 | 10.8 | 5.5 | 0.20 | 89 | 1.2 | 8.0 | 9.4 | 7.1 | 2.5 | 0.438 | 0.055 | 12.2 | 13.1 | 31.2 | 0.6 | −5.11 | 13 | 129 | 4.38 | 0.71311 |
| G6 | 2.45 | 10 | 11.0 | 4.85 | 0.14 | 239 | 0.1 | 21.3 | 15.8 | 28.1 | 6.3 | 5.13 | 0.127 | 8.2 | 44.7 | 102.1 | 0.1 | −6.02 | 11 | 221 | 3.24 | 0.71230 |
| G8 | 12.20 | 14 | 11.1 | 4.8 | 0.07 | 393 | 10 | 15.3 | 15.1 | 48.8 | 17.6 | 0.076 | 0.290 | 4.0 | 33.7 | 60.9 | 189.5 | −6.18 | 12 | 168 | 4.52 | 0.71321 |
| G9 | 3.70 | 10 | 10.5 | 4.5 | 0.04 | 173 | 0.1 | 15.8 | 3.1 | 13.0 | 6.6 | 10.3 | 0.115 | 2.4 | 30.3 | 83.1 | 0.2 | −7.57 | 13 | 113 | 5.11 | 0.71363 |
| G10 | 2.35 | 8 | 12.4 | 4.5 | 0.08 | 390 | 0.2 | 34.1 | 92.7 | 12.3 | 4.5 | 0.317 | 0.055 | 4.9 | 72.3 | 75.1 | 86.7 | −7.25 | 10 | 224 | 2.07 | 0.71147 |
| AB1 | 2.70 | 20 | 10.9 | 5.3 | 0.31 | 349 | 0.1 | 29.0 | 44.3 | 21.6 | 11 | 11.5 | 0.237 | 18.6 | 58.8 | 145.8 | 0.8 | −4.93 | 15 | 91 | 5.24 | 0.71372 |
| AB2 | 2.50 | 26 | 10.9 | 6.1 | 0.63 | 309 | 0.1 | 20.6 | 4.8 | 33.6 | 9.2 | 22.4 | 0.171 | 38.1 | 42.5 | 128.2 | 0.2 | −2.96 | 12 | 196 | 2.04 | 0.71145 |
| AB3 | 1.45 | 30 | 10.8 | 7.55 | 3.58 | 403 | 0.2 | 75.3 | 2.3 | 28.7 | 2.5 | 1.22 | 0.091 | 218.4 | 29.9 | 33.4 | 0.4 | −0.33 | 4 | 315 | −1.80 | 0.70872 |
| AB4 | 4.10 | 54 | 11.4 | 7.52 | 1.32 | 172 | 0.1 | 9.3 | 1.2 | 21.7 | 3.3 | 11.5 | 0.051 | 80.5 | 14.1 | 21.4 | <0.1 | −0.85 | <0.6 | 425 | −0.85 | 0.70940 |
| AB5 | 2.95 | 29 | 10.7 | 5.75 | 0.33 | 224 | 0.1 | 17.8 | 10.2 | 24.6 | 8.7 | 5.03 | 0.161 | 20.1 | 39.1 | 90.6 | 0.1 | −3.96 | 12 | 153 | 2.86 | 0.71203 |
| AB6 | 2.45 | 25 | 10.7 | 6.0 | 0.47 | 282 | 0.2 | 25.0 | 4.9 | 37.2 | 8.7 | 5.83 | 0.194 | 28.4 | 43.5 | 119 | 0.5 | −3.21 | 17 | 192 | −0.75 | 0.70947 |
| AB8 | 12.20 | 17 | 11.3 | 5.25 | 0.12 | 278 | 6.3 | 18.7 | 4.0 | 40.0 | 9.5 | 0.327 | 0.154 | 7.3 | 38.5 | 56.9 | 95.1 | −5.10 | 9 | 260 | 0.75 | 0.71053 |
| AB9 | 3.80 | 21 | 10.5 | 6.75 | 1.29 | 217 | 0.3 | 10.3 | 1.0 | 35.0 | 2.9 | 6.86 | 0.071 | 78.4 | 25.5 | 43.8 | 0.5 | −1.60 | 4 | 493 | −1.07 | 0.70924 |

[a] BSS = below soil surface; ALK = alkalinity; TDS = total dissolved solids, n.d. = not determined.
[b] Saturation indices with respect to calcite (SI$_{cc}$) were modeled using PHREEQC (Parkhurst and Appelo, 1999).
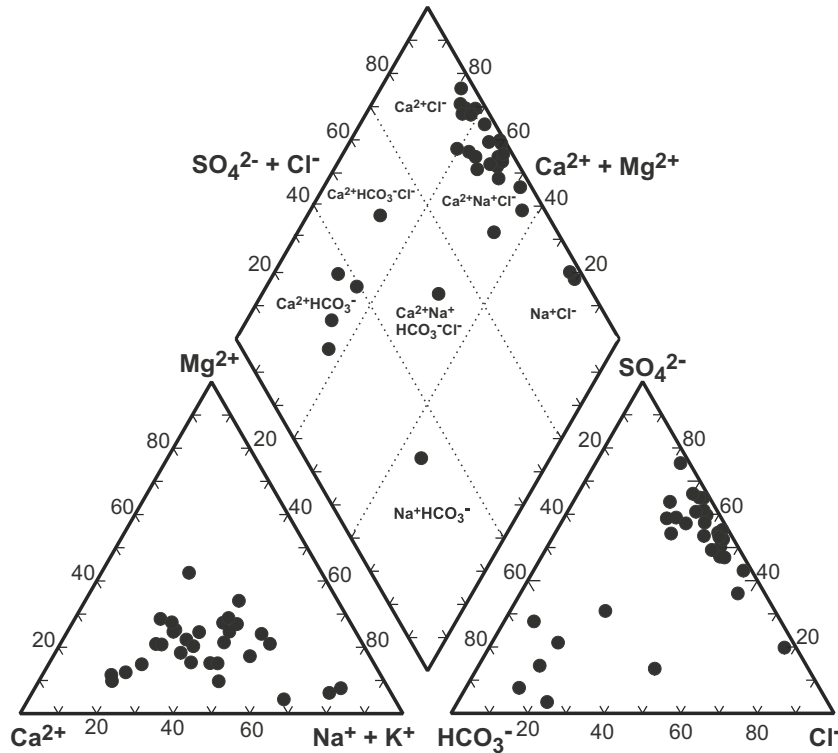[c] $\delta^{87}Sr$ values are normalized to rainwater ($^{87}Sr/^{86}Sr = 0.710$).

**Fig. 2.** Characterization of groundwater in diagrams after Piper (1944). Most groundwater samples have Ca–Na–Cl-, Ca–Cl- (shallow depths), and Ca–HCO$_3$-type compositions (deep wells).

result of exhaustion in dissolved oxygen due to organic matter degradation. In contrast, oxic groundwater is prevalent in the southwestern part of the aquifer (Geest plain), where monitoring wells contain high nitrate concentrations up to 190 mg/L NO$_3^-$. At reducing groundwater conditions nitrate concentrations decrease to values below detection limits due to denitrification processes. Anoxic groundwater of the Weser marshland and deeper aquifer horizons are typically enriched in SO$_4^{2-}$ and in dissolved Fe up to 22 mg/L due to reductive processes.

In shallow depths (<20 m BSS), groundwater is characterized by Ca–Na–Cl- and Ca–Cl-type compositions, whereas Ca–HCO$_3$-type groundwater prevails in deep wells (>30 m BSS) (Fig. 2). Intermediate groundwater depths (20–30 m BSS) are characterized either by Ca–Na–Cl-, Ca–Cl, or Ca–HCO$_3$-type compositions. Decalcification of soils produces low alkalinity and undersaturation of groundwater with respect to calcite. Both pH values and alkalinity of groundwater increase with depth. At neutral pH value groundwater is close to equilibrium with calcite. Parallel to the distribution of pH, saturation indices for calcite (SI$_{calcite}$) vary from −7.57 in shallow to −0.33 in deep wells.

Tritium concentrations and stable isotopes of oxygen and hydrogen indicate modern recharge during the past about 50 years for shallow to intermediate groundwater wells. In those wells, tritium concentrations average 16 ± 7 TU ($n = 19$; year 2001). In deep wells (54 m BSS), tritium concentrations were below detection limits, indicating that deep groundwater was recharged before ∼1950. The distribution of stable oxygen and hydrogen isotopes show no influence of Pleistocene groundwater; $\delta^{18}$O and $\delta$D values plot along a local meteoric water line according to the equation: D = 7.37 $^{18}$O + 2.11 ($R^2$ = 0.93) (Fig. 3).

### $\delta^{87}$Sr values and Ca/Sr ratios in precipitation and groundwater

The average $^{87}$Sr/$^{86}$Sr ratio of local precipitation is 0.710 equal to a $\delta^{87}$Sr value of "0" (Wiegand et al., 2001). This value is in the
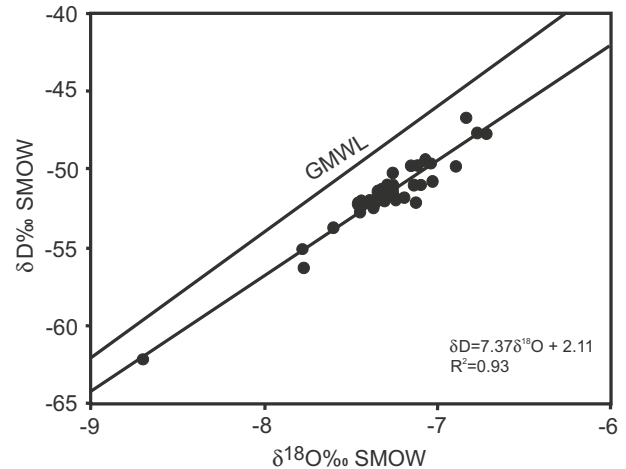


**Fig. 3.** Distribution of $\delta^{18}$O and $\delta$D (normalized to SMOW) in groundwater. $\delta^{18}$O and $\delta$D values plot along a local meteoric water line according to the equation: $\delta$D = 7.37 $^{18}$O + 2.11. The global meteoric water line (GMWL) is added as a reference.

range of $^{87}$Sr/$^{86}$Sr ratios analyzed for rainwater at other European locations, e.g. Chabaux et al. (2005), Négrel et al. (2007). Concentrations of Sr$^{2+}$ in precipitation average 3 μg/L, resulting in rainwater-derived Sr$^{2+}$ inputs to the catchment of approximately 2 mg/m$^2$ yr$^{-1}$. Dissolved Sr$^{2+}$ concentrations in groundwater range from 50 to 300 μg/L with $\delta^{87}$Sr values between 7.3 and −2.6 (Table 1). Sr$^{2+}$ concentrations do not show a systematic distribution across the aquifer, however, $\delta^{87}$Sr values vary with depth, pH value, Ca/Sr ratio, and calcite saturation index (SI$_{calcite}$). In shallow depths, positive $\delta^{87}$Sr values are evolved, whereas $\delta^{87}$Sr values decline below the value of local precipitation in deeper groundwater horizons (Fig. 4). Parallel, pH values increase from 4.4 in shallow to
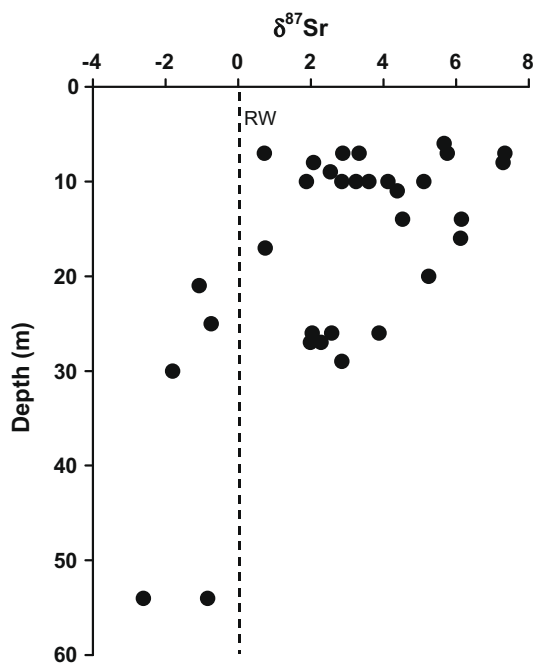
**Fig. 4.** Depth-related distribution of $\delta^{87}Sr$ values in groundwater. $\delta^{87}Sr$ of rainwater (RW) is given as a reference line. Depth in meters below soil surface (BSS).
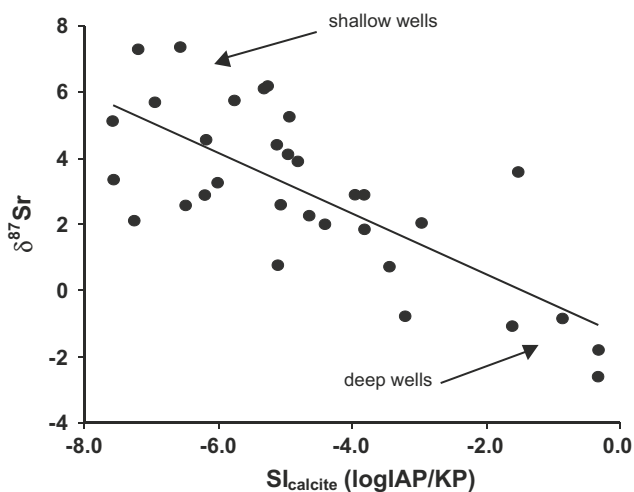


**Fig. 5.** Distribution of $\delta^{87}Sr$ relative to saturation indices for calcite ($SI_{calcite}$) in groundwater. Strong undersaturation with respect to calcite corresponds with positive $\delta^{87}Sr$ values; higher $SI_{calcite}$ values are associated with negative $\delta^{87}Sr$ values; [$\delta^{87}Sr = -0.92 \, SI - 1.34$; $R^2 = 0.55$].

7.6 in deep wells, and both parameters are inversely correlated ($R^2$: 0.55). The changes in pH and $\delta^{87}Sr$ values indicate significant changes in the weathering conditions and the sources of base cations contributing to the dissolved loads. Positive $\delta^{87}Sr$ values account for higher contributions from weathering silicate minerals in shallow depths, while negative $\delta^{87}Sr$ values of deep groundwater are linked to dissolution of/or equilibrium with calcium carbonate. Accordingly, $\delta^{87}Sr$ and $SI_{calcite}$ values are significantly correlated ($R^2$: 0.55) (Fig. 5).

Further geochemical fingerprints like the Ca/Sr ratio may be used to distinguish between dissolving carbonate and silicate phases. Ca/Sr ratios of groundwater range from 88 to 493 and are negatively correlated with $\delta^{87}Sr$ values ($R^2$: 0.62). Weathering of Ca-poor silicate minerals produces low Ca/Sr ratios, while high

Ca/Sr ratios are associated with the dissolution of calcium carbonate. Ca/Sr ratios and $\delta^{87}Sr$ values are independent tracers and the correlation of both in the present study provides a reliable means to distinguish sources of Sr and Ca.

### Distribution of $\delta^{87}Sr$ in sediment and minerals

The aquifer is mainly composed of coarse to fine-grained quartz sand ($SiO_2 > 90\%$) that contains variable amounts of accessory minerals including glauconite, feldspar, mica, and calcium carbonate. Trace amounts of illite are present in deeper sediment horizons. Gravel (partly from Nordic crystalline rocks), boulder clay, and organic layers are locally intercalated. $\delta^{87}Sr$ values of bulk sediment from the unsaturated and saturated zones vary between 28 and 65 with an average of $45 \pm 1$ ($n = 36$) (Table 2). In the unsaturated zone, $\delta^{87}Sr$ values generally increase with depth, while for the saturated zone a decrease to a $\delta^{87}Sr$ value of 42 can be observed in depths between 25 and 30 m BSS (sediment profile B16; Table 2). Highest $\delta^{87}Sr$ values (51–65) are associated with layers of course sand and fine gravel, while low $\delta^{87}Sr$ values (35–42) correspond with fine-grained sand and silt horizons e.g. in the unsaturated and shallow saturated zones and in deeper horizons between 20 and 30 m depth.

While Sr isotope analyses of bulk sediment contribute to understanding mineralogical heterogeneities in the aquifer on a larger scale, mineral separates allow direct determination of the dissolving phases that govern the Sr isotope composition of the dissolved pool. Quartz, the predominant mineral contains extremely low amounts of Sr, thus contributing only little to the isotopic composition of the bulk sediment and the dissolved pool (Rossman et al., 1987). Consequently, the Sr isotope composition of the bulk sediment is controlled by the distribution of accessory mineral phases, which represent mixtures from silicates and carbonates in different quantities. Analyses of mineral separates yield the following $\delta^{87}Sr$ values (Table 2): 18.3 (glauconite), 33.8 (feldspar: the feldspar separate contains a mixture of K-feldspar and plagioclase; separation between the two phases was not possible due to the small grain size and intense weathering of the minerals), 133.5 (muscovite), and 296.3 (biotite, partly chloritized). Glauconite and feldspar have $\delta^{87}Sr$ values below the average of bulk sediment, while micas contribute more radiogenic Sr. In addition, calcium carbonate (mostly disperse, occasionally small fragments of limestone and marine fossils) is a supplier of non-radiogenic Sr especially in deep aquifer horizons. Both glauconite and calcium carbonate are presumably derived from underlying Late Cretaceous and Tertiary deposits that were reworked during the Pleistocene glaciations. $\delta^{87}Sr$ values of Late Cretaceous and Tertiary limestones vary between −3.1 and −1.8 (Burke et al., 1982; Smalley et al., 1994). For comparison, the most negative $\delta^{87}Sr$ value analyzed for groundwater in 54 m BSS is −2.6.

Ca concentrations of the bulk sediment are variable with highest values in deeper aquifer horizons. The unsaturated zone contains between 400 and 1600 mg/kg Ca with an average of $876 \pm 321$ mg/kg, and between 24 and 58 mg/kg Sr with an average of $40 \pm 9$ mg/kg. In the saturated zone, average Ca concentrations increase by a factor of two to $2091 \pm 68$ mg/kg in depths below 19 m. Higher Ca concentrations are usually associated with smaller grain sizes <200 μm, suggesting that the amount of disperse calcium carbonate is elevated in fine-grained deep aquifer horizons. In sediment profile B16 Sr concentrations ($39 \pm 5$ mg/kg) vary little and Ca/Sr ratios increase from an average of 22 in the unsaturated zone to 52 below 19 m BSS. Low Ca/Sr ratios indicate silicate-rich/carbonate-poor sediments, while the increase in Ca/Sr ratios is associated with the increasing calcium carbonate content in deeper aquifer horizons.

Additional sources of Ca in near-surface sediment and shallow groundwater may include Ca-rich fertilizer and decomposing

**Table 2**
$\delta^{87}Sr$ and Ca/Sr data of sediment profiles from the unsaturated and saturated zones.

| Sample ID | Sampling depth (m) | Analyzed fraction | Aquifer zone | Ca (mg/kg) | Sr (mg/kg) | Ca/Sr | $\delta^{87}Sr$ | $^{87}Sr^{86}Sr$ |
|---|---|---|---|---|---|---|---|---|
| 1.5 | 1.07 | BS | UZ | 1644 | 49 | 34 | 30 | 0.73107 |
| 1.13 | 2.78 | BS | UZ | 786 | 28 | 28 | 60 | 0.75259 |
| 2.6 | 1.2 | BS | UZ | 1215 | 49 | 25 | 52 | 0.74718 |
| 2.9 | 1.74 | BS | UZ | 786 | 32 | 25 | 54 | 0.74825 |
| 3.5 | 1.0 | BS | UZ | 572 | 33 | 17 | 50 | 0.74571 |
| 3.10 | 2.06 | BS | UZ | 572 | 34 | 17 | 51 | 0.74603 |
| 3.21 | 4.84 | BS | UZ | 572 | 39 | 15 | 49 | 0.74489 |
| 5.2 | 0.51 | BS | UZ | 1001 | 34 | 29 | 38 | 0.73722 |
| 5.6 | 1.19 | BS | UZ | 1144 | 48 | 24 | 32 | 0.73278 |
| 5.8 | 1.67 | BS | UZ | 1287 | 58 | 22 | 34 | 0.73414 |
| 8.5 | 1.23 | BS | UZ | 500 | 24 | 21 | 47 | 0.74343 |
| 8.17 | 3.54 | BS | UZ | 1001 | 48 | 21 | 37 | 0.73648 |
| 10.3 | 0.71 | BS | UZ | 1144 | 38 | 30 | 48 | 0.74375 |
| 11.3 | 1.08 | BS | UZ | 643 | 41 | 16 | 37 | 0.73647 |
| 11.5 | 1.43 | BS | UZ | 643 | 44 | 15 | n.d. | n.d. |
| 11.7 | 1.70 | BS | UZ | 572 | 30 | 19 | 57 | 0.75029 |
| 14.4 | 1.28 | BS | UZ | 1072 | 55 | 19 | 28 | 0.73000 |
| 14.6 | 1.77 | BS | UZ | 429 | 33 | 13 | 34 | 0.73448 |
| B16 | 0.4–0.9 | BS | UZ | 858 | 36 | 24 | 37 | 0.73622 |
| B16 | 4–5 | <200 µm | UZ | 1072 | 45 | 24 | 42 | 0.73950 |
| B16 | 6–7 | BS | SZ | 572 | 30 | 19 | 46 | 0.74260 |
| B16 | 6–7 | <200 µm | SZ | 1001 | 42 | 24 | n.d. | n.d. |
| B16 | 8–9 | <200 µm | SZ | 1644 | 42 | 39 | 51 | 0.74624 |
| B16 | 11–12 | BS | SZ | 929 | 32 | 29 | 56 | 0.74960 |
| B16 | 12–13 | <200 µm | SZ | 2216 | 45 | 49 | 52 | 0.74687 |
| B16 | 14–15 | BS | SZ | 1358 | 40 | 34 | 65 | 0.75639 |
| B16 | 19–20 | BS | SZ | 2144 | 43 | 50 | 51 | 0.74635 |
| B16 | 24–25 | <200 µm | SZ | 2073 | 40 | 52 | 43 | 0.74081 |
| B16 | 28–29 | BS | SZ | 2144 | 40 | 54 | 42 | 0.74008 |
| B16 | 28–29 | <200 µm | SZ | 2001 | 38 | 53 | n.d. | n.d. |
| Rainwater | | Average | $n = 5$ | 1.22 | 0.003 | 407 | 0 | 0.71017 |
| Feldspar[c] | | | | 4952 | 195 | 25 | 34 | 0.73352 |
| Glauconite | | | | 5847 | 49 | 119 | 18 | 0.72250 |
| Muscovite | | | | n.d. | n.d. | n.d. | 133 | 0.80477 |
| Biotite (chloritized) | | | | n.d. | n.d. | 22–33[b] | 296 | 0.92034 |
| CaCO$_3$ | | Average[a] | | 400000 | 400 | 1000 | −2.96 | 0.70790 |

Abbreviations: BS = bulk sediment; UZ = unsaturated zone; SZ = saturated zone; n.d. = not determined.

[a] Average Sr concentration of Cretaceous limestone (after Demovic and Wedepohl, in Hoefs, 1970) $\delta^{87}Sr$ ratios of cretaceous limestone: −1.8 to −3.1 (after Burke et al., 1982; Smalley et al., 1994); $\delta^{87}Sr$ = −2.96 was used for model calculations.

[b] Ca/Sr ratio of biotite; data from Taylor et al. (2000) and Gunter et al. (1993).

[c] The feldspar separate contains a mixture of alkali feldspar and plagioclase.

organic matter, which has incorporated Sr from atmospheric sources (e.g. Wiegand et al., 2005). Those sources may contribute to the non-radiogenic Sr pool, resulting in a decrease in $\delta^{87}Sr$ values of sediment and groundwater in shallow horizons. Ca-rich fertilizers usually contain Ca from marine limestone/dolomite, thus negative $\delta^{87}Sr$ values are expected. Commercially available fertilizers were studied by e.g. Böhlke and Horan (2000), Soler et al. (2002), and Vitòria et al. (2004), resulting in $\delta^{87}Sr$ values between −2.8 and −1.4 and Ca/Sr ratios that overlap with potential marine calcium carbonate sources in the investigated catchment. Organic fertilizer (manure) contains Sr mostly from local crops that match the plant available Sr pool.

## Discussion

### Constraining sources of dissolved $Sr^{2+}$

Sources of $Sr^{2+}$ in groundwater reflect mixtures of atmospheric, lithogenic, and potentially anthropogenic inputs. The $\delta^{87}Sr$ value of rainwater equals "0" (see "Methods" and "$\delta^{87}Sr$ values and Ca/Sr ratios in precipitation and groundwater"), silicate phases have positive $\delta^{87}Sr$ values between 18 and 296, and marine carbonates (including Ca-containing fertilizers) are characterized by negative $\delta^{87}Sr$ values between −1.4 and −3.1. In most near-surface wells, the Sr isotopic composition of the dissolved pool is more radio-

genic than the infiltrating rainwater due to contributions from weathering silicate phases. A decrease in $\delta^{87}Sr$ in deep wells below the rainwater-introduced Sr isotope value reflects the predominance of $Sr^{2+}$ from calcium carbonate.

Although quartz is the dominant mineral in the aquifer, both low Sr concentrations and low dissolution rates (e.g. Rossman et al., 1987; Brady and Walther, 1990; House and Hickinbotham, 1992; Dove, 1995) suggest only insignificant contributions to the dissolved pool. Lithogenic $Sr^{2+}$ inputs are therefore controlled by accessory mineral phases. Experimental dissolution rates of primary minerals are usually in the order calcite–hornblende–plagioclase–biotite–K-feldspar–muscovite–quartz (Berner and Berner, 1987). Biotite and hornblende are largely depleted from the soil column, and trace amounts of chloritized biotite (0.1%) suggest only a minor influence on the Sr isotope composition of groundwater. It is possible that biotite mostly disintegrated during glacial transport (Anderson et al., 1997; Anderson, 2005). Under glacial conditions, weathering of biotite and depletion of $K^+$ and radiogenic $Sr^{2+}$ from interlayer sites is known to be rapid (e.g. Drever and Hurcomb, 1986; Blum et al., 1994; Taylor et al., 2000). The depletion of biotite in the aquifer may reflect significant glacial weathering. From the silicate phases present, feldspars are the most likely source for radiogenic Sr in the dissolved pool due to their relatively high dissolution rates. Glauconite, as a member of the clay mineral group, is assumed to have a high weathering resistance and low dissolution rates may be expected in the range of
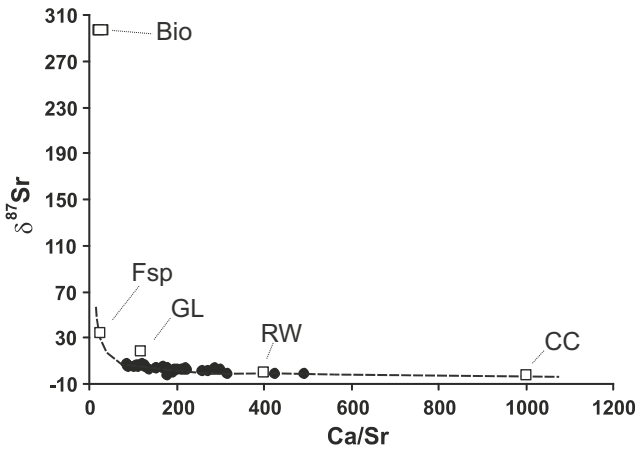
**Fig. 6.** Distribution of $\delta^{87}$Sr and Ca/Sr ratios in groundwater (closed circles) ($R^2 = 0.62$), rainwater (RW), calcium carbonate (CC), feldspar (Fsp), biotite (Bio), and glauconite (GL) (rainwater/mineral data displayed as open squares).

muscovite and quartz. However, release of interlayer cations including $Sr^{2+}$ may affect groundwater composition at acidic conditions (e.g. Bau et al., 2004; Fernandez-Bastero et al., 2008).

To constrain contributing sources, the relationship between $\delta^{87}$Sr values and Ca/Sr ratios of groundwater samples, rainwater, biotite, feldspar, glauconite, and calcium carbonate was evaluated (Fig. 6). Both rainwater and calcium carbonate are characterized by high Ca/Sr ratios and non-radiogenic Sr isotope compositions, while the analyzed biotite and feldspar separates are characterized by high $\delta^{87}$Sr values and low Ca/Sr ratios. Glauconite has a lower Sr isotope composition than the other silicate phases and a Ca/Sr ratio that overlaps with Ca/Sr in groundwater samples.

Feldspar and calcium carbonate are considered to be the main sources of dissolved $Sr^{2+}$ and $Ca^{2+}$ in groundwater. Radiogenic $Sr^{2+}$ contributions from biotite are assumed to be of minor significance because of the strong depletion of biotite in the sediment. Also, glauconite is likely not a significant source for $Sr^{2+}$ due to its high weathering resistance and a four times lower Sr concentration than feldspar. Though, small contributions from interlayer sites cannot be completely excluded for shallow groundwater that is characterized by low pH values.

The position of the groundwater samples proximate to the end-members rainwater, feldspar, and calcium carbonate suggests that the dissolved $Sr^{2+}$ and $Ca^{2+}$ pools are mainly derived by a mixture of those sources. Because of low solute concentrations in rainwater, the release of $Sr^{2+}$ from mineral weathering predominates the $\delta^{87}$Sr isotope signal in groundwater. Feldspar dissolution dominates contributions from silicate weathering, though feldspar-derived $Sr^{2+}$ inputs are estimated to be small compared to inputs from calcium carbonate sources (sources include weathering of carbonate minerals and possible fertilizer inputs). This finding is in agreement with lower $Sr^{2+}$ and $Ca^{2+}$ concentrations in feldspar compared to calcium carbonate and a higher dissolution rate of the latter.

*Evolution of groundwater and mixing calculations*

Proportional contributions from the sources calcium carbonate, feldspar, biotite, and rainwater can be modeled using $\delta^{87}$Sr values and $Sr^{2+}$ concentrations according to the following Eqs. (2)–(5). The average $Sr^{2+}$ concentration in local precipitation is 3 µg/L, and average annual precipitation and recharge rates are 691 mm and 200 mm, respectively (see see "Methods" and "$\delta^{87}$Sr values and Ca/Sr ratios in precipitation and groundwater"). Assuming steady state conditions concerning recharge/discharge and constant aver-

age inputs from atmospheric precipitation during the time of groundwater formation for shallow to intermediate depths (during the past about 50 years or less according to tritium concentrations in groundwater of >8 TU), the concentration of rainwater-derived $Sr^{2+}$ entering the groundwater cycle is about 11 µg/L. Deducting the amount of rainwater-derived $Sr_r$ from the analyzed $Sr^{2+}$ concentration in groundwater ($Sr_w$) determines the contribution of mineral weathering-derived $Sr_m$. The resulting change in $\delta^{87}Sr_m$ can be computed according to

$$\delta^{87}Sr_m = \frac{(\delta^{87}Sr_w \times Sr_w) - (\delta^{87}Sr_r \times Sr_r)}{Sr_m} \tag{2}$$

The contribution from mineral weathering consists of a mixture from biotite, feldspar, and calcium carbonate. As discussed earlier ("Constraining sources of dissolved $Sr^{2+}$"), biotite is strongly depleted in the aquifer, and constitutes ~0.1% of the reactive silicate phases. Radiogenic $Sr^{2+}$ supplied to the groundwater by biotite is calculated based on the estimated abundance. To determine weathering contributions from feldspar ($Sr_f$) and calcium carbonate ($Sr_k$), the following 2-component mixing calculation is employed (Eq. (3)). (Note: the feldspar fraction contains a mixture of both plagioclase and alkali feldspar which were considered together.)

$$Sr_m \times \delta^{87}Sr_m = (Sr_m - Sr_f) \times \delta^{87}Sr_k + Sr_f \times \delta^{87}Sr_f \tag{3}$$

The amount of feldspar-derived $Sr_f$ in groundwater can be obtained by converting Eq. (3) to (4).

$$Sr_f = \frac{Sr_m \times \delta^{87}Sr_m - Sr_m \times \delta^{87}Sr_k}{\delta^{87}Sr_f - \delta^{87}Sr_k} \tag{4}$$

The concentration of carbonate-derived $Sr_k$ is obtained by subtracting the amount of feldspar-derived $Sr_f$ from the bulk weathering-derived accumulation

$$Sr_k = Sr_m - Sr_f \tag{5}$$

Fig. 7 displays the distribution of modeled $Sr^{2+}$ inputs from atmospheric and mineral weathering sources relative to groundwater depth. Contributions from feldspars reach 8–26% in shallow to intermediate groundwater wells, while rainwater and calcium carbonate provide 4–20% and 62–90%, respectively. The amount of biotite-derived radiogenic $Sr^{2+}$ was calculated to 0.1% for shallow to deep wells. Groundwater of some intermediate and deep wells (below 20 m BSS) contain between 95% and 99.8% of calcium carbonate-derived $Sr^{2+}$, and less than 5% from feldspars. Because groundwater from those wells is close to equilibrium with calcite and not (considerably) affected by modern recharge (tritium concentrations are between 4 TU and <0.6 TU), rainwater-derived $Sr^{2+}$ was assumed negligible and not considered in the mixing calculation.

Lithogenic inputs from silicate and carbonate weathering provide more than 80% of dissolved $Sr^{2+}$ in groundwater, while contributions from rainwater are relatively small with an average of 8% due to low solute concentrations in atmospheric precipitation. Both $Sr^{2+}$ inputs from feldspars and calcium carbonate show significant correlations with the pH value of groundwater as a result of the pH dependence of the weathering reactions (Fig. 8). Feldspar weathering is enhanced at acidic conditions in decalcified shallow to intermediate aquifer horizons, and decreases with aquifer depths when disperse calcium carbonate buffers groundwater acidity and pH values rise. At neutral pH, feldspar dissolution is minor, while equilibrium with calcium carbonate controls groundwater chemistry and the supply of dissolved $Sr^{2+}$. The observed pH dependence of feldspar dissolution is in agreement with experimental results, e.g. by Helgeson et al. (1984), Knauss and Wolery (1986), Murphy and Helgeson (1987).
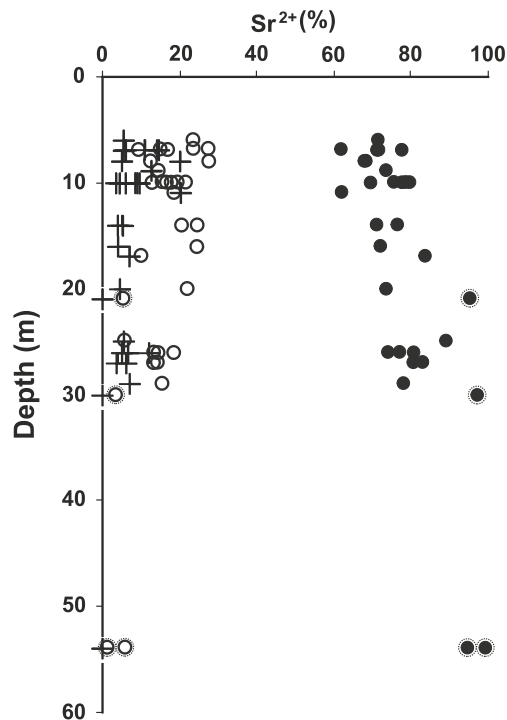
**Fig. 7.** Depth-related distribution of modeled $Sr^{2+}$ (%) contributions from atmospheric precipitation (cross symbols), feldspars (open circles), and calcium carbonate (closed circles) to groundwater. Groundwater samples that are close to equilibrium with calcite are marked by dotted circles.
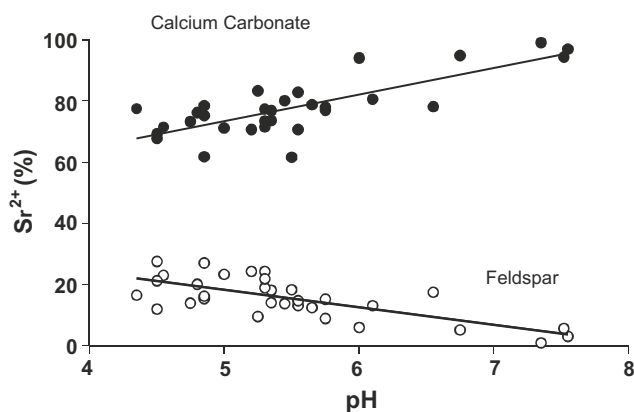


**Fig. 8.** Proportions of dissolved $Sr^{2+}$ (%) released from feldspar (open circles; $R^2$: 0.52) and calcium carbonate (closed circles; $R^2$: 0.62) in relation to pH values of groundwater. The dissolution of feldspar is enhanced at acidic pH in decalcified aquifer horizons.

Though feldspar is a significant suppliers of radiogenic $Sr^{2+}$ in groundwater of shallow to intermediate depths, on average 75% of the dissolved pool is controlled by non-radiogenic $Sr^{2+}$ inputs from calcium carbonate sources. As a result, $Ca^{2+}$ concentrations of calcite-undersaturated groundwater are positively correlated with the amount of carbonate-derived $Sr^{2+}$ ($R^2 = 0.62$). The high content of carbonate-derived $Sr^{2+}$ in groundwater associated with the decalcified part of the aquifer is likely linked to contributions from Ca–N-rich fertilizers. In the NW German Geest, lime-marl and Ca-containing fertilizers were traditionally used in agriculture to improve soil fertility. High nitrate concentrations (avg. 52 mg/L; $n = 14$) in oxic groundwater are characteristic for the intense use of fertilizers in the catchment area during the past dec-

ades. Carbonate-derived $Sr^{2+}$ introduced to the investigated aquifer by fertilizer application is indistinguishable from local calcium carbonate sources by means of Sr isotope analysis (see Distribution of $\delta^{87}Sr$ in sediment and minerals). Thus, proportions of $Sr^{2+}$ from fertilizer cannot be quantified.

## Conclusions

Decalcification of silicate-dominated soils has a significant impact on chemical weathering and solute sources in shallow unconfined aquifers. Sr isotope ratios, Ca/Sr, and hydrochemical data provide distinctive fingerprints to discriminate and quantify solute contributions of lithogenic and atmospheric origin and thus assist in evaluating effects of decalcification on vulnerable groundwater resources. Depletion of calcium carbonate in the upper sediment column of the investigated catchment causes a significant decrease in the acid-neutralization capacity and consequently low pH values in groundwater that trigger accelerated silicate weathering. Modern groundwater in shallow to intermediate aquifer depths is strongly undersaturated with respect to calcite, and dissolving feldspars are the predominant silicate source providing radiogenic $Sr^{2+}$ and low Ca/Sr ratios. Considerable amounts of non-radiogenic $Sr^{2+}$ in groundwater of decalcified horizons suggest an origin in Ca-containing fertilizers that were introduced to the catchment by intensive agricultural land use. Lithogenic inputs from silicates (feldspars, biotite) and calcium carbonate supply more than 80%, while atmospheric precipitation contributes ⩽20% of dissolved $Sr^{2+}$ and $Ca^{2+}$ to shallow and intermediate groundwaters. In deeper located calcareous sediments, calcium carbonate governs non-radiogenic $\delta^{87}Sr$ values and high Ca/Sr ratios of the dissolved pool. Lithogenic contributions exceed 95% from calcium carbonate and less than 5% from feldspars. Equilibrium with calcium carbonate is restricted to old groundwater sources that are essentially tritium-free. No modern groundwater has achieved equilibrium with calcite due to the strong depletion of calcium carbonate in shallow to intermediate aquifer depths. Trends in groundwater pH, saturation indices with respect to calcite, and the distribution of $\delta^{87}Sr$ values suggest that large parts of the aquifer above 30 m BSS are decalcified. Assuming that decalcification of the sediment has intensified over the past decades due to the anthropogenic impact, the equilibrium between groundwater and calcium carbonate has been affected irreversibly in shallow to intermediate aquifer depths of the investigated catchment.

## Acknowledgements

## References

Åberg, G., 1995. The use of natural Sr isotopes as tracers in environmental studies. Water Air Soil Pollut. 79, 309–322.

Anderson, S.P., 2005. Glaciers show direct linkage between erosion rate and chemical weathering fluxes. Geomorphology 67, 147–157.

Anderson, S.P., Drever, J.I., Humphrey, N.F., 1997. Chemical weathering in glacial environments. Geology 25, 399–402.

Bau, M., Alexander, B., Chesley, J.T., Dulski, P., Brantley, S.L., 2004. Mineral dissolution in the Cape Cod aquifer, Massachusetts, USA: I reaction stoichiometry and impact of accessory feldspar and glauconite on strontium

isotopes, solute concentrations, and REY distribution. Geochim. Cosmochim. Acta 68, 1199–1216.

Berner, E.K., Berner, R.A., 1987. The Global Water Cycle: Geochemistry and Environment. Prentice-Hall, Inc.,, Englewood Cliffs, NJ. pp. 142–155.

Blum, J.D., Erel, Y., Brown, K., 1994. $^{87}Sr/^{86}Sr$ ratios of Sierra Nevada stream waters: implications for relative mineral weathering rates. Geochim. Cosmochim. Acta 58, 5019–5025.

Böhlke, J.K., Horan, M., 2000. Strontium isotope geochemistry of groundwaters and streams affected by agriculture, Locust Grove, MD. Appl. Geochem. 15, 599–609.

Brady, P.V., Walther, J.V., 1990. Kinetics of quartz dissolution at low temperatures. Chem. Geol. 82, 253–264.

Brantley, S.L., Chesley, J.T., Stillings, L.L., 1998. Isotopic ratios and release rates of strontium measured from weathering feldspars. Geochim. Cosmochim. Acta 62, 1493–1500.

Bricker, O.P., Rice, K.C., 1993. Acid Rain. Annu. Rev. Earth Planet. Sci. 21, 151–174.

Bullen, T.D., Krabbenhoft, D.P., Kendall, C., 1996. Kinetic and mineralogic controls on the evolution of groundwater chemistry and $^{87}Sr/^{86}Sr$ in a sandy silicate aquifer, northern Wisconsin. Geochim. Cosmochim. Acta 60, 1807–1821.

Bullen, T., White, A., Blum, A., Harden, J., Schulz, M., 1997. Chemical weathering of a soil chronosequence on granitoid alluvium: II mineralogic and isotopic constraints on the behavior of strontium.. Geochim. Cosmochim. Acta 61, 291–306.

Burke, W.H., Denison, R.E., Hetherington, E.A., Koepnik, R.B., Nelson, N.F., Otto, J.B., 1982. Variation of seawater $^{87}Sr/^{86}Sr$ throughout phanerozoic time. Geology 10, 516–519.

Capo, R.C., Stewart, B.W., Chadwick, O.A., 1998. Strontium isotopes as tracers of ecosystem processes: theory and methods. Geoderma 82, 197–225.

Chabaux, F., Riotte, J., Schmitt, A.D., Carignan, J., Herckes, P., Pierret, M.C., Wortham, H., 2005. Variations of U and Sr isotope ratios in Alsace and Luxembourg rain waters: origin and hydrogeochemical implications. Comptes Rendus Geosci. 337, 1447–1456.

Dahl, H.-J., Dörhöfer, G., 1991. Grundwasser in Niedersachsen. Akademie für Geowissenschaften und Geotechnologien, Heft 7, Schweizbart, Stuttgart, Germany, 118p.

Dörhöfer, G., Kunkel, R., Tetzlaff, B., Wendland, F., 2001. Der natürliche Grundwasserhaushalt in Niedersachsen. In: Aufbruch nach Europa – Hydrogeologie vor neuen Aufgaben. Der natürliche Grundwasserhaushalt in Niedersachsen, Arbeitshefte – Wasser, vol. 1, 109–167.

Dove, P.M., 1995. Kinetic and thermodynamic controls on silica reactivity in weathering environments. In: White, A.F., Brantley, S.L. (Eds.), Chemical Weathering Rates of Silicate Minerals. Rev. Mineral., vol. 31, pp. 235–290.

Drever, J.I., Hurcomb, D.R., 1986. Neutralization of atmospheric acidity by chemical weathering in an alpine drainage basin in the North Cascades Mountains. Geology 14, 221–224.

Driscoll, C.T., Lawrence, G.B., Bulger, A.J., Butler, Y.J., Eagar, C., Lambert, K.F., Likens, G.E., Stoddard, J.L., Weathers, K.C., 2001. Acidic deposition in the Northeastern United States: sources and inputs, ecosystem effects, and management strategies. Bioscience 51, 180–198.

EG-WRRL Report, 2005. Niedersächsisches Landesamt für Bodenforschung (NLfB) Niedersächsisches Landesamt für Ökologie (NLÖ), Bericht 2005, Grundwasser Stand 15.07.2004, Betrachtungsraum NI05 – Mittlere Weser, Ergebnisse der Bestandsaufnahme, Land Niedersachsen, http://www.wrrl-kommunal.de/seiten/umsetzung/bestandsaufnahme_2004/downloads/c-berichte_gw/Weser/C-Bericht_GW_Mittlere_Weser.pdf.

Ehlers, J., Meyer, K.-D., Stephan, H.-J., 1984. The pre-Weichselian glaciations of North-West Europe. Quat. Sci. Rev. 3, 1–40.

Eissmann, L., 2002. Quaternary geology of eastern Germany (Saxony, Saxon-Anhalt, South Brandenburg, Thuringia), type area of the Elsterian and Saalian Stages in Europe. Quaternary Sci. Rev. 21, 1275–1346.

Falkengren-Grerup, U., Linnermark, N., Tyler, G., 1987. Changes in the acidity and cation pools of south Swedish soils between 1949 and 1985. Chemosphere 16, 2239–2248.

Fenn, M.E., Huntington, T.G., McLaughlin, S.B., Eagar, C., Gomez, A., Cook, R.B., 2006. Status of soil acidification in North America. J Forensic Sci. 52, 3–13 (special issue).

Fernandez-Bastero, S., Gil-Lozano, C., Briones, M.J.I., Gago-Duport, L., 2008. Kinetic and structural constraints during glauconite dissolution: implications for mineral disposal of $CO_2$. Mineral. Mag. 72, 27–31.

Grube, F., Christensen, S., Vollmer, T., Duphorn, K., Klostermann, J., Menke, B., 1986. Glaciations in north west Germany. In: Šibrava, V. et al. (Eds.), Quaternary Glaciations in the Northern Hemishpere. Quatern. Sc. Rev., vol. 5, pp. 347–358.

Gunter, M.E., Johnson, N.E., Knowles, C.R., Solie, D.N., 1993. A Rb–Sr isochron from a single biotite crystal. Mineral. Mag. 57, 746–749.

Helgeson, H.C., Murphy, W.M., Aagaard, P., 1984. Thermodynamic and kinetic constraints on reaction rates among minerals and aqueous solutions II. Rate constants, effective surface area, and the hydrolysis of feldspar. Geochim. Cosmochim. Acta 48, 2405–2432.

Hoefs, J., 1970. Kohlenstoff- und Sauerstoff-Isotopenuntersuchungen an Karbonat-konkretionen und umgebendem Gestein (Mit einem Anhang über Strontiumgehalte dieser Proben von Demovic, R. Und Wedepohl, K.H.). Contruct. Mineral. Petrol. 27, 66–79.

House, W.A., Hickinbotham, L.A., 1992. Dissolution kinetics of silica between 5 and 35 °C. J. Chem. Soc. Faraday Trans. 88, 2021–2026.

Hrkal, Z., Prchalova, H., Fottova, D., 2006. Trends in impact of acidification on groundwater bodies in the Czech Republic; an estimation of atmospheric deposition at the horizon 2015. J Atmosph. Chem. 53, 1–12.

Huntington, T.G., Hooper, R.P., Johnson, C.E., Aulenbach, B.T., Cappelato, R., Blum, A.E., 2000. Calcium depletion in a southeastern United States forest ecosystem. Soil Sci. Soc. Am. J. 6, 1845–1858.

Jacobson, A.D., Blum, J.D., Chamberlain, C.P., Poage, M.A., Sloan, V.F., 2002. Ca/Sr and Sr isotope systematics of a Himalayan glacial chronosequence: carbonate versus silicate weathering rates as a function of landscape surface age. Geochim. Cosmochim. Acta 66, 13–27.

Johnson, T.M., DePaolo, D.J., 1994. Interpretation of isotopic data in groundwater-rock systems: model development and application to strontium isotope data from Yucca Mountain. Water Resources Res. 30, 1571–1587.

Katz, B.G., Bullen, T.D., 1996. The combined use of $^{87}Sr/^{86}Sr$ and carbon and water isotopes to study the hydrochemical interaction between groundwater and lakewater in mantled karst. Geochim. Cosmochim. Acta 60, 5075–5087.

Kartenserver des NIBIS, 2008a. Geologische Karte von Niedersachsen und Bremen 1:25 000 (Blatt 3018 Syke/Blatt 3019 Weyhe), Landesamt für Bergbau, Energie und Geologie (LBEG), Hannover, Germany.

Kartenserver des NIBIS, 2008b. Durchlässigkeiten der oberflächennahen Gesteine (1:500 000), Landesamt für Bergbau, Energie und Geologie (LBEG), Hannover, Germany.

Knauss, K.G., Wolery, T.J., 1986. Dependence of albite dissolution kinetics on pH and time at 25 °C and 70 °C. Geochim. Cosmochim. Acta 50, 248l–2497.

Lawrence, G.B., David, M.B., Lovett, G.M., Murdoch, P.S., Burns, D.A., Stoddard, J.L., Baldigo, B.P., Porter, J.H., Thompson, A.W., 1999. Soil calcium status and the response of stream chemistry to changing acidic deposition rates in the Catskill Mountains of New York. Ecol. Appl. 9, 1059–1072.

Likens, G.E., Driscoll, C.T., Buso, D.C., 1996. Long-term effects of acid rain: responses and recovery of a forest ecosystem. Science 272, 244–246.

Meyer, K., 2005. Zur Stratigraphie des Saale-Glazials in Niedersachsen und zu Korrelationsversuchen mit Nachbargebieten In: Eiszeitalter und Gegenwart, vol. 55, pp. 25–42.

Miller, E.K., Blum, J.D., Friedland, A.J., 1993. Determination of soil exchangeable-cation loss and weathering rates using Sr isotopes. Nature 362, 438–441.

Murphy, W.M., Helgeson, H.C., 1987. Thermodynamic and kinetic constraints on reaction rates among minerals and aqueous solutions. III Activated complexes and the pH-dependence of the rates of feldspar, pyroxene, wollastonite, and olivine hydrolysis. Geochim. Cosmochim. Acta 51, 3137–3153.

Négrel, P., Guerrot, C., Millot, R., 2007. Chemical and strontium isotope characterisation of rainwater in France. Isot. Environ. Health Stud. 43, 179–196.

Négrel, P., Petelet-Giraud, E., Widory, D., 2004. Sr isotope geochemistry of alluvial groundwater: a tracer for groundwater resources characterisation. Hydrol. Earth Syst. Sci. 8, 959–972.

Parkhurst, D.L., Appelo, C.A.J., 1999. User's guide to PHREEQC (version 2) – a computer program for speciation, batch-reaction, one-dimensional transport, and inverse geochemical calculations. US Geol. Survey. Water-Resour. Inv. Rep. 99-4259, 312p.

Peterman, Z.E., Wallin, B., 1999. Synopsis of strontium isotope variations in groundwater at Äspö, southern Sweden. Appl. Geochem. 14, 939–951.

Piper, A.M., 1944. A graphic procedure in the geochemical interpretation of water analyses. AGUTrans. 25, 914–923.

Probst, A., El Gh'mari, A., Aubert, D., Fritz, B., McNutt, R., 2000. Strontium as a tracer of weathering processes in a silicate catchment polluted by acid atmospheric inputs, Strengbach. France. Chem. Geol. 170, 203–219.

Quade, J., English, N., DeCelles, P.G., 2003. Silicate versus carbonate weathering in the Himalaya: a comparison of the Arun and Seti River watersheds. Chem. Geol. 202, 275–296.

Rossman, G.R., Weis, D., Wasserburg, G.J., 1987. Rb, Sr, Nd and Sm concentrations in quartz. Geochim. Cosmochim. Acta 51, 2325–2329.

Shand, P., Darbyshire, D.P.F., Gooddy, D., Haria, A.H., 2007. $^{87}Sr/^{86}Sr$ as an indicator of flowpaths and weathering rates in the Plynlimon experimental catchments, Wales, UK. Chem. Geol. 236, 247–265.

Shortle, W.C., Bondietti, E.A., 1992. Timing, magnitude, and impact of acidic deposition on sensitive forest sites. Water Air Soil Pollut. 61, 253–267.

Smalley, P.C., Higgins, A.C., Howarth, R.J., Nicholson, H., Jones, C.E., Swinburne, N.H.M., Bessa, J., 1994. Seawater Sr isotope variations through time: a procedure for constructing a reference curve to date and correlate marine sedimentary rocks. Geology 22, 431–434.

Soler, A., Canals, A., Goldstein, S.L., Otero, N., Antich, N., Spangenberg, J., 2002. Sulfur and strontium isotope composition of the Llobregat river (NE Spain): tracers of natural and anthropogenic chemicals in stream waters. Water Air Soil Pollut. 236, 207–224.

Sposito, G., 1989. The Chemistry of Soils. Oxford University Press, New York. 277 pp..

Taylor, A.S., Blum, J.D., Lasaga, A.C., MacInnis, I.N., 2000. Kinetics of dissolution and Sr release during biotite and phlogopite weathering. Geochim. Cosmochim. Acta 64, 1191–1208.

Vitòria, L., Otero, N., Soler, A., Canals, À., 2004. Fertilizer Characterization: Isotopic Data (N, S, O, C and Sr). Environ. Sci. Technol. 38, 3254–3262.

Walter, R., 2007. Geologie von Mitteleuropa, seventh ed. Schweizbart, Stuttgart, Germany. 511 p.

Wiegand, B., Dietzel, M., Bielert, U., Groth, P., Hansen, B.T., 2001. $^{87}Sr/^{86}Sr$-Verhältnisse als Tracer für geochemische Prozesse in einem Lockergesteinsaquifer (Liebenau, NW-Deutschland). Acta Hydrochim. Hydrobiol. 29, 139–152.

Wiegand, B.A., Chadwick, O.A., Vitousek, P.M., Wooden, J.L., 2005. Ca cycling and isotopic fluxes in forested ecosystems in Hawaii. Geophys. Res. Lett. 32 (Art. no. L11404).